

648 **Intentional Gesture: Deliver your Intentions with Gestures for Speech**

649

650

651

652

653

Supplementary Material

A OVERVIEW

654

The supplementary material is organized into the following sections:

656

- Section B: Additional Dataset Analysis
- Section C: Annotation Protocol and Validation
- Section D: Implementation Details
- Section E: Additional Experiments
- Section F: User Study Details
- Section G: Metric Details
- Section H: Ethical Statement
- Section I: Reproducibility statement
- Section J: The Use of Large Language Models
- Section K: Limitations

657

658

659

660

661

662

663

664

665

666

667

668

669 For more visualization, please see the additional demo videos.

670

B ADDITIONAL DATASET ANALYSIS

671

B.1 FUNCTION-TO-GESTURE MAPPING GROUNDING

672

673 Our function-to-gesture mappings derive from established frameworks in gesture pragmatics,
 674 particularly McNeill McNeill (1992) and Kendon Kendon (2004). Tab. 5 presents gesture forms
 675 associated with each communicative function, which inform our VLM annotation prompt’s gesture
 676 behavior mapping.

677

678 Certain functions correspond to consistent physical gestures (e.g., Deixis to pointing, Emphasis
 679 to beat gestures, Negation to head shakes), while others like Modal or Mental State manifest
 680 in subtler movements (fist tightening, shoulder shrugs). These literature-backed correspondences
 681 ensure interpretable and plausible annotations, providing a bridge between gesture generation and
 682 discourse semantics.

683

684 Tab. 5 shows the function distribution across dataset splits. Core functions such as Deixis (57-61%),
 685 Emphasis (46-51%), Mental State (41%), and Process (26-29%) are well-represented with minimal
 686 variation across splits. Less frequent functions like Comparison, Modal, and Valence (5-8%) and
 687 specialized functions (Intensifier, Physical Relation, 1%) show distributional consistency. Note that
 688 these percentages reflect per-sentence function occurrence rather than the cumulative distribution
 689 reported in the main paper.

690

B.2 CO-OCCURRENCE PATTERNS AND SPEAKER-SPECIFIC GESTURE PROFILES.

691

692 To further examine the structure of our function annotations, we analyze co-occurrence patterns
 693 and speaker-level gesture usage. Figures 8(a-c) present conditional co-occurrence heatmaps for the
 694 top 8 gesture functions across train, validation, and test splits. Each cell reflects the probability
 695 that function j co-occurs given function i within the same utterance. We observe strong mutual
 696 co-occurrence between Emphasis and Deixis, as well as between Mental State and Emphasis,
 697 suggesting these functions often emerge in jointly expressive speech segments. These co-occurrence
 698 trends remain stable across dataset splits, reinforcing the semantic consistency of our annotations.

699

700

701

702 Figure 8(d) shows a radar plot of gesture function usage for the top 6 most frequent speakers. While
 703 some functions like Deixis and Emphasis are commonly expressed across speakers, other functions
 704 (e.g., Contrast, Modal, Quantification) exhibit speaker-specific variability. This aligns with prior

702 Table 5: Gesture function statistics and mappings. For each function, we report its relative frequency
 703 (%) across dataset splits and its typical gestural manifestation.

704

| 705 Function | 706 Frequency (%) | | | 707 Typical Gesture Mapping |
|------------------------|-------------------|----------|----------|---|
| | 708 Train | 709 Val | 710 Test | |
| 711 Deixis | 712 57.3 | 713 61.8 | 714 60.2 | 715 Index finger pointing, gaze direction shift |
| 716 Emphasis | 717 48.3 | 718 50.6 | 719 46.4 | 720 Beat gestures, small head nods |
| 721 Mental State | 722 42.0 | 723 41.1 | 724 41.1 | 725 Shrug, slow head tilt, hand on chest |
| 726 Process | 727 29.1 | 728 25.6 | 729 28.8 | 730 Circular motion, continuous hand movement |
| 731 Quantification | 732 16.7 | 733 20.6 | 734 17.0 | 735 Spread fingers, repeated motions |
| 736 Spatial Relation | 737 16.1 | 738 16.5 | 739 18.2 | 740 Hands indicating space or depth |
| 741 Negation | 742 13.2 | 743 12.3 | 744 11.0 | 745 Head shake, subtle hand wave |
| 746 Affirmation | 747 8.9 | 748 10.7 | 749 9.9 | 750 Big nod, repeated nods |
| 751 Valence | 752 8.1 | 753 7.0 | 754 7.1 | 755 Open hands (positive), recoiling motion (negative) |
| 756 Modal | 757 7.6 | 758 8.1 | 759 5.2 | 760 Tight fist, upward palm with tension |
| 761 Comparison | 762 6.6 | 763 7.7 | 764 5.6 | 765 Left-right hand sweep, comparative spacing |
| 766 Interrogative | 767 4.6 | 768 2.9 | 769 3.4 | 770 Raised eyebrows, open palms |
| 771 Contrast | 772 3.9 | 773 3.5 | 774 3.2 | 775 Alternating hand gestures, lateral head tilt |
| 776 Intensifier | 777 1.4 | 778 1.4 | 779 1.2 | 780 Sharp eyebrow raise, large gesture amplitude |
| 781 Performance Factor | 782 1.0 | 783 1.1 | 784 0.9 | 785 Gaze aversion, short blink, pause gestures |
| 786 Physical Relation | 787 0.6 | 788 0.6 | 789 0.7 | 790 Gesture showing size/shape (e.g., distance between hands) |

791 Figure 8: **Co-occurrence and speaker-level analysis of gesture function annotations.** (a–c)
 792 show conditional co-occurrence heatmaps of the top 8 gesture functions across the train, validation,
 793 and test splits, respectively. Each cell indicates the probability of function j appearing given
 794 function i (i.e., $P(j|i)$). Strong pairings (e.g., Emphasis + Deixis, Mental State + Emphasis) reveal
 795 compositional gesture semantics. (d) presents radar plots of function distribution across the top 6
 796 speakers, revealing shared trends (e.g., high Deixis usage) and speaker-specific variation in gesture
 797 behavior.

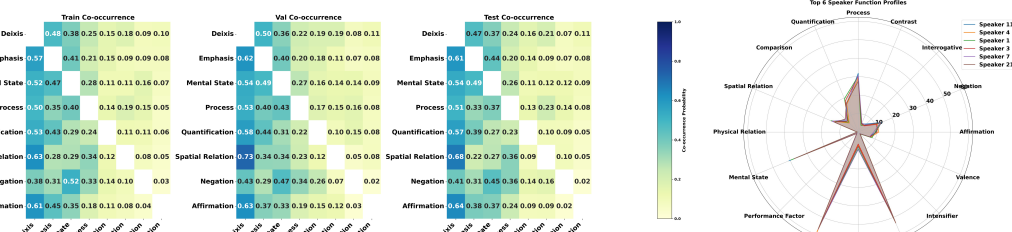
(a)

(b)

(c)

(d)

798 findings that gesture behavior reflects both discourse demands and speaker idiosyncrasies Kendon
 799 (2004). Such variation presents a valuable modeling challenge for systems that aim to personalize
 800 or adapt gesture generation to individual styles.



Algorithm 1 Motion Pattern Detection

Require: Input data $\mathbf{y} \in \mathbb{R}^T$, thresholds ϵ_s, ϵ

Ensure: Motion statistics and extrema relations

- 1: $\mathbf{y} \leftarrow$ reshape to 1D array
- 2: **if** $T \leq 1$ **then return** insufficient_data
- 3: **end if**
- 4: // Extract key statistics
- 5: $y_0, y_T \leftarrow \mathbf{y}[0], \mathbf{y}[T - 1]$
- 6: $i_{max}, i_{min} \leftarrow \arg \max(\mathbf{y}), \arg \min(\mathbf{y})$
- 7: $y_{max}, y_{min} \leftarrow \mathbf{y}[i_{max}], \mathbf{y}[i_{min}]$
- 8: $\delta \leftarrow y_{max} - y_{min}, \Delta \leftarrow y_T - y_0$
- 9: // Check if motion is static
- 10: **if** $\delta < \epsilon_s$ **then**
- 11: **return** {pattern: ‘linear’, range: δ , direction: $\text{sign}(\Delta)$ }
- 12: **end if**
- 13: // Compute extrema relations
- 14: $\mathbf{s} \leftarrow [|y_0 - y_{max}| \leq \epsilon, |y_0 - y_{min}| \leq \epsilon]$ ▷ Start position
- 15: $\mathbf{e} \leftarrow [|y_T - y_{max}| \leq \epsilon, |y_T - y_{min}| \leq \epsilon]$ ▷ End position
- 16: $\mathbf{in} \leftarrow [i_{max} \notin \{0, T-1\}, i_{min} \notin \{0, T-1\}]$ ▷ Interior extrema
- 17: **return** { $\mathbf{y}, \Delta, \delta, \mathbf{s}, \mathbf{e}, \mathbf{in}$ }

Algorithm 2 Motion Pattern Classification

Require: Extrema relations $\mathbf{s} = [s_{max}, s_{min}]$, $\mathbf{e} = [e_{max}, e_{min}]$, $\mathbf{in} = [in_{max}, in_{min}]$

Ensure: Pattern type and description

- 1: **if** $(s_{max} \wedge e_{min}) \vee (s_{min} \wedge e_{max})$ **then** ▷ Opposite extremes
- 2: pattern \leftarrow ‘round_trip’
- 3: **else if** $(s_{max} \vee s_{min}) \wedge (e_{max} \vee e_{min})$ **then** ▷ Same extreme
- 4: pattern \leftarrow ‘return_to_extreme’
- 5: **else if** $(s_{max} \vee s_{min}) \wedge \neg(e_{max} \vee e_{min})$ **then** ▷ Leave from extreme
- 6: pattern \leftarrow ‘peak_at_start’
- 7: **else if** $(e_{max} \vee e_{min}) \wedge \neg(s_{max} \vee s_{min})$ **then** ▷ Arrive at extreme
- 8: pattern \leftarrow ‘peak_at_end’
- 9: **else if** $in_{max} \wedge in_{min}$ **then** ▷ Both extremes inside
- 10: pattern \leftarrow ‘peak_between’
- 11: **else if** $in_{max} \oplus in_{min}$ **then** ▷ One extreme inside
- 12: pattern \leftarrow ‘single_extreme_inside’
- 13: **else** ▷ Boundary-aligned
- 14: pattern \leftarrow ‘complex_extrema’
- 15: **end if**
- 16: **return** pattern

Algorithm 3 Helper Functions

- 1: **function** GETDIRECTION(Δ)
- 2: **return** $\begin{cases} \text{‘positive’} & \text{if } \Delta > 0 \\ \text{‘negative’} & \text{if } \Delta < 0 \\ \text{‘none’} & \text{otherwise} \end{cases}$
- 3: **end function**
- 4: **function** CLASSIFYMOVEMENT($\Delta, \epsilon_s, \epsilon_{slow}$)
- 5: **return** $\begin{cases} \text{‘static’} & \text{if } |\Delta| < \epsilon_s \\ \text{‘slow’} & \text{if } |\Delta| < \epsilon_{slow} \\ \text{‘significant’} & \text{otherwise} \end{cases}$
- 6: **end function**

810
811
812
813
814 **Table 6: Training-time annotation prompt with visual grounding.** Our framework analyzes
815 human gestures by integrating visual keyframes with speech.
816
817

818 **System Prompt:**
819 Assume you are the annotator for human gestures. Given images for each word the person speaks, you
820 need to provide fine-grained analysis from motion captions, to Function Derivations, Gesture Behavior
821 Mapping, and finally Inferred Intention. The Definition of Function Derivation & Gesture Behavior
822 Mapping are as follows:
823
824

825 [Function Derivation: 16 classes of Function Derivations]
826 [Gesture Behavior Mapping: How functions map to physical movements.]
827
828

829 **User Prompt:**
830 I will provide you with a transcript of speech, the atomic pose angle movement descriptions and
831 corresponding images showing the speaker’s gestures. Please analyze the motion and provide a detailed
832 description as the generation output following this format:
833
834

835 [Format Instruction]
836

837 **Motion Analysis:**

- 838 • **Head:** Describe head movements (nodding, shaking, tilting)
- 839 • **Hands & Fingers:** Describe hand gestures, positions, finger articulations
- 840 • **Arms & Shoulders:** Describe arm movements and shoulder positions
- 841 • **Legs & Feet:** Describe lower body movements and weight shifts
- 842 • **Torso & Whole Body:** Describe posture and body orientation

843 **Function Derivation:** List relevant functions from the prior knowledge

844 **Gesture Behavior Mapping:** Map each function to observed gestures

845 **Inferred Intention:** Explain overall communicative intent

846 [One-shot Example:]
847

848 **Input:** “I think this one is much better than the previous one.” [Images]

849 **Output:** Motion Analysis: [Head, hands, arms, legs, body movements]

850 Function Derivation: [Comparison, Emphasis, Deixis functions]

851 Gesture Behavior Mapping: [Function-to-gesture relationships]

852 Inferred Intention: [Communication intent analysis]

853 [Data to be Annotated]
854
855

856 **C ANNOTATION PROTOCOL AND VALIDATION**

857 **C.1 MOTION PATTERN ANALYSIS**

858 We propose a rule-based algorithm for classifying temporal motion patterns by analyzing the
859 geometric relationships between trajectory extrema and boundaries. Given a motion sequence
860 $y \in \mathbb{R}^T$ (e.g., joint angles or hand positions), our method extracts key statistics and determines
861 the motion pattern through a deterministic decision process, as detailed in Algorithms 1–2.

862 The algorithm operates in three stages. First, it computes fundamental statistics: boundary values
863 (y_0, y_T), global extrema (y_{\max}, y_{\min}) with their indices, and the motion range $\delta = y_{\max} - y_{\min}$
864 (Algorithm 1, lines 3–6). If δ falls below a static threshold ϵ_s , the motion is classified as linear/static,
865 avoiding misclassification of noise as complex patterns (Algorithm 1, lines 8–10).

866 For non-static motion, the algorithm analyzes **extrema-boundary relations** by computing boolean
867 indicators for whether the start/end positions are near (within tolerance ϵ) the global extrema, and
868 whether extrema occur in the trajectory interior (Algorithm 1, lines 12–14). These geometric
869 relations capture motion characteristics invariant to scale and translation.

870 Finally, pattern classification applies hierarchical logical rules based on these relations (Algo-
871 rithm 2). For instance, if the trajectory starts near one extreme and ends near the opposite
872 ($s_{\max} \wedge e_{\min}) \vee (s_{\min} \wedge e_{\max}$), it’s classified as a “round trip” pattern (Algorithm 2, lines 2–3). Other

864
 865
 866
Table 7: Test-time annotation prompt without visual grounding. To prevent data leakage in
 867 evaluation, test-time annotations deliberately exclude visual information, requiring functions and
 868 intentions to be inferred solely from linguistic content.
 869

870 **System Prompt:**
 871 Assume you are the annotator for human speech. Without access to gesture images, you need to infer likely
 872 communicative functions and intentions from linguistic content alone. Based on Function Derivations,
 873 analyze the words and its durations within the transcript. Then analyze the Inferred Intention. The
 874 Definition of Function Derivation are as follows:
 875
 876 [Function Derivation: 16 classes of Function Derivations]
 877
 878 **User Prompt:**
 879 I will provide you with:
 880 • Previous two sentences for context
 881 • Current sentence to be annotated
 882 • *No visual information or keyframes*
 883 Please analyze the linguistic content and provide predictions as follows:
 884
 885 **Linguistic Analysis:**
 886 • Identify key words and phrases that typically trigger gestures
 887 • Note speech elements that commonly correlate with specific movements
 888 • Analyze the syntactic and semantic structure that implies gesture potential
 889 **Function Derivation:** Infer likely functions based solely on linguistic content
 890 **Predicted Gesture Types:** Suggest probable gesture categories without seeing actual movements
 891 **Inferred Intention:** Predict the likely communicative intent based on linguistic cues
 892
 893 [One-shot Example for In-Context Learning without visual data]
 894 [Data to be Annotated - transcript only]

895 patterns include “return to extreme” (starting and ending at the same extreme), “peak between” (both
 896 extrema in the interior), and “single extreme inside” (one interior extreme), among others.
 897

898 The algorithm employs context-aware thresholds that adapt based on motion type (e.g., different sen-
 899 sitivity for hand positions vs. joint angles) and achieves $\mathcal{O}(T)$ complexity through efficient single-
 900 pass operations (Algorithm 2). This deterministic approach provides interpretable pattern detection
 901 without requiring training data, making it suitable for real-time motion analysis applications where
 902 understanding the type of movement (cyclic, monotonic, or complex) is crucial for downstream
 903 tasks.

901 C.2 TRAINING-TIME ANNOTATION PROTOCOL (WITH MOTION FRAMES)

902 To construct training annotations, we prompt GPT-4o-mini with both linguistic and visual inputs.
 903 Each prompt includes: (1) The two previous sentences spoken by the speaker, serving as linguistic
 904 context. (2) The current sentence to annotate, segmented into word units with corresponding
 905 timestamps. (3) The sampled starting and ending keyframe image for each word, together with
 906 the rule-based motion description annotation for the poses. We show the prompt template in Tab.6.
 907 The model is instructed to generate a structured analysis with the following outputs:

908 **Motion Analysis:** Detailed natural language description of body movements, including head
 909 motion, arm/shoulder gestures, finger positions, torso orientation, and stance.

910 **Function Derivation:** Identification of pragmatic functions (e.g., Emphasis, Deixis, Negation) that
 911 are linguistically relevant to the current sentence.

912 **Gesture Behavior Mapping:** Mapping between derived functions and observable gesture types
 913 (e.g., pointing, nodding, brow raise) following established gesture theory.

914 **Inferred Intention:** A communicative goal inferred from the alignment of motion and function
 915 (e.g., emphasizing contrast, directing attention, expressing uncertainty).

918
 919
 920
 921
 922
 923 **Table 8: Baseline annotation prompt without structure.** This naive protocol excludes gesture
 924 theory or function derivation, asking the model to directly infer the speaker’s communicative intent.
 925 This leads to overgeneralized or underspecified outputs.
 926
 927

928 **System Prompt:**

929 You are an assistant that helps interpret the meaning behind a speaker’s body language and words. Given
 930 the speaker’s sentence and gesture images for each word, describe what the speaker is trying to express
 931 overall. Do not break the task into components; simply provide an intention summary based on what you
 932 perceive.
 933

934 [No prior gesture theory, no function derivation definitions]

935 **User Prompt:**

936 I will give you:

- 937 • A transcript of the speaker’s sentence
- 938 • An image for each word the speaker says

939 Please describe what the speaker is trying to express or communicate. Use natural language, and focus on
 940 the overall message or feeling you perceive.

941 **Output:**

- 942 • One or two sentences summarizing the speaker’s communicative intention
- 943 • Do not perform motion breakdown or gesture labeling
- 944 • Do not mention gesture function classes or mappings

945 [Example:]

946 **Input:** “I think this one is much better than the previous one.” [Images]

947 **Output:** The speaker is expressing a strong preference for a current choice, likely implying confidence or
 948 satisfaction.

949 [Data to be Annotated]

950 This protocol captures visually grounded, multi-level annotation aligned with both motion and
 951 speech.
 952

953 **C.3 TEST-TIME ANNOTATION PROTOCOL (TRANSCRIPT ONLY)**

954 To avoid potential data leakage in test annotations, we exclude visual motion input from the VLM
 955 prompts during test set annotation. Each test prompt contains the two prior sentences for context
 956 and the current sentence to be annotated. No keyframes or motion descriptions are provided. The
 957 VLM is instructed to: (1) Infer likely communicative functions based solely on linguistic content.
 958 (2) Derive high-level communicative intent without visual grounding, as shown in Tab.7.

959 This simulates the actual evaluation scenario, where gesture models must predict motion solely from
 960 speech, and prevents the test set annotations from being conditioned on ground-truth poses.
 961

962 **C.4 BASELINE ANNOTATION PROTOCOL (NO STRUCTURED PROMPT)**

963 To examine the importance of structured reasoning, we design a baseline annotation protocol that
 964 omits the function derivation and gesture behavior mapping stages. In this setting, GPT-4o-mini is
 965 prompted with the current sentence and visual frames for each word, but is asked only to provide
 966 an inferred intention directly—without performing intermediate motion analysis or reasoning about
 967 communicative function. We present the prompt example in Tab.8.

968 This resembles a generic captioning-style instruction (e.g., “Describe what the speaker is trying to
 969 express”), lacking any prior definitions or decomposition of gesture semantics. While this setup may
 970 yield fluent outputs, it often results in: (1) **Overgeneralization:** Outputs tend to collapse nuanced
 971 signals (e.g., emphasis, negation, deixis) into vague descriptions such as “the speaker is sharing
 972 a thought.” (2) **Hallucination:** In the absence of reasoning stages, the model may infer incorrect
 973 intentions (e.g., persuasive intent where none exists). (3) **Loss of Interpretability:** Since outputs
 974 are not grounded in functional structure, they cannot be mapped to gesture execution in a controllable
 975 or compositional way. This baseline highlights the necessity of structured prompting in generating

972 **Table 9: Comparative annotation outputs across two utterances.** Structured annotations include
 973 function derivation and gesture mapping. Improper annotations suffer from overgeneralization,
 974 hallucination, or lack of compositionality.
 975

| Utterance A: "I think watching anime is helpful for me" | |
|---|--|
| 977 Training-Time (w/ 978 motion) | 979 Function Derivation: <i>Deixis</i> ("me"), <i>Mental State</i> (positive belief). 980 Gesture Mapping: Deixis → hand at chest, Mental State → relaxed stance. 981 Inferred Intention: The speaker reflects personally on the benefit of anime. 982 Gestures reinforce introspection and confidence. |
| 983 Test-Time (transcript-only) | 984 Function Derivation: <i>Deixis, Mental State</i> . 985 Gesture Mapping: [Not available] 986 Inferred Intention: The speaker shares a personal viewpoint with implied 987 conviction, likely supported by subtle gestures. |
| 988 Improper: Flat In- 989 tent Only | 990 Inferred Intention: The speaker is talking about anime. 991 <i>[Missing: No function derivation, no motion context, no gestural insight.]</i> |
| 992 Improper: Halluci- 993 nated Purpose | 994 Inferred Intention: The speaker is encouraging the audience to try watching anime 995 as a productivity tool. <i>[Issue: Adds persuasive intent not supported by transcript or body motion.]</i> |
| 996 Improper: Misaligned Gesture 997 Mapping | 998 Inferred Intention: The speaker is contrasting anime with something unhelpful. <i>[Issue: Misinterprets positive reflection as contrast/negation.]</i> |
| Utterance B: "I always try to move as much as I can when I'm not working" | |
| 999 Training-Time (w/ 1000 motion) | 1001 Function Derivation: <i>Emphasis</i> ("working"), <i>Negation</i> ("not working"), <i>Modal</i> 1002 ("can"). Gesture Mapping: Emphasis → steady hands reinforce commitment; Negation → 1003 assertive fist posture; Modal → gestural space around "can". 1004 Inferred Intention: Speaker emphasizes an active lifestyle outside of work. 1005 Gestures signal assertion and capability. |
| 1006 Test-Time (transcript-only) | 1007 Function Derivation: Same as above (<i>Emphasis, Negation, Modal</i>). 1008 Gesture Mapping: [Omitted] 1009 Inferred Intention: The speaker frames movement as a conscious, empowering 1010 action. Likely gestures reinforce contrast and agency. |
| 1011 Improper: Flat In- 1012 tent Only | 1013 Inferred Intention: The speaker is saying that they move around a lot. <i>[Issue: No deeper intent, no gesture mapping, missing compositional structure.]</i> |
| 1014 Improper: 1015 Misaligned Functions | 1016 Inferred Intention: The speaker is unsure whether they move enough and seems 1017 to compare working vs. resting. <i>[Issue: Misses clear assertion and negation. Misreads modality.]</i> |
| 1018 Improper: No Com- 1019 position | 1020 Inferred Intention: The speaker likes to be active. <i>[Issue: Oversimplifies the sentence; collapses nuanced components (modal vs. 1021 negation vs. emphasis) into a flat label.]</i> |

1022 interpretable and semantically grounded gesture annotations. We include comparative examples in
 1023 Tab. 9 to illustrate these failure modes in context.

1024 C.5 ANNOTATION VALIDATION AND HUMAN PREFERENCE STUDY

1025 To assess the reliability of our annotation pipeline, we randomly sampled 100 utterances from the
 1026 training set. Each sample was annotated using both the training protocol (with-motion) and the test
 1027 protocol (transcript-only). Separately, expert annotators were provided with: (1) The utterance and
 1028 its transcript. (2) The full sequence of rendered motion frames.

1029 Experts then independently labeled: (1) The communicative function(s) present. (2) The inferred
 1030 intention based on motion and speech. (3) The gesture types observed in the motion.

1031 We then presented annotators with three candidate annotations for each sample (training VLM, test
 1032 VLM, and human-generated), blinded and randomized. Annotators were asked to rate: (1) Which

1026 annotation most accurately reflected the speaker’s intent. **(2)** Which annotation was most clearly
 1027 and consistently reasoned.

1028 Results, shown in main paper Fig.4, indicate that the training-style annotation (with visual grounding)
 1029 achieved the highest human preference. However, the transcript-only test-style annotations
 1030 also achieved strong scores, outperforming human-generated annotations in clarity and structural
 1031 alignment. This validates the effectiveness of our prompt design and supports the use of VLM-
 1032 generated labels for both training and evaluation.

1034 C.6 VLM CONSISTENCY AND HALLUCINATION AUDIT

1036 To ensure the reliability of our VLM-based annotation pipeline, we performed two targeted sanity
 1037 checks: a consistency audit and a hallucination spot check.

1039 **Consistency Under Repeated Prompts.** We randomly selected 100 utterances from the dataset
 1040 and re-prompted GPT-4o-mini three times each under the same configuration. We examined the
 1041 stability of the output across three categories: (i) function derivations, (ii) inferred intentions, and
 1042 (iii) gesture behavior mappings. Across the 300 trials: 93% of the outputs maintained consistent
 1043 function derivation labels. 84% preserved consistent gesture mappings across trials. These results
 1044 suggest that the model exhibits stable behavior under repeated prompting, with low variance in the
 1045 output of structural annotations.

1047 **Hallucination Spot Check.** To assess the faithfulness of annotation outputs to visual evidence,
 1048 we conducted an expert spot check on 50 randomly sampled annotation instances. Each instance
 1049 included three components: **(1) Motion Descriptionz**, **(2) Function–Gesture Mapping**, and **(3)**
 1050 **Inferred Intention**. For motion descriptions, 4 out of 50 samples (8%) were flagged for partial
 1051 inconsistencies. These typically involved subtle over-interpretations—e.g., stating a “brow raise”
 1052 when the face appeared neutral in the keyframe. No instances of fully fabricated or unrelated
 1053 gestures were identified. For Function–Gesture Mapping, only 1 sample (2%) was marked as
 1054 problematic, where a mapping relation (e.g., from a deictic phrase to a pointing gesture) was missing.
 1055 The issue stemmed from under-specification rather than misalignment. For intention inference,
 1056 3 samples (6%) were flagged for slight exaggerations—such as over-interpreting neutral tones as
 1057 emphasizing emotion. These were still broadly reasonable within the context of the utterance,
 1058 and none were deemed to be outright hallucinations. Overall, the hallucination rate was low, and
 1059 all identified issues were minor and recoverable. Importantly, no samples exhibited completely
 1060 incorrect reasoning or disjointed alignment. This suggests the annotations are well-grounded and
 1061 highlights the strong prompt-following and contextual inference abilities of the VLM. We also
 1062 observe that minor hallucinations in motion description do not meaningfully degrade the accuracy
 1063 of intention inference, supporting the robustness of our pipeline.

1064 C.7 HUMAN STUDY INSTRUCTIONS

1066 We present the details how we conducted the manual hallucination checking from the users as
 1067 follows.

1069 **Study 1: Function–Gesture Mapping Coherence Objective:** Evaluate whether gestures are
 1070 appropriate and coherent realizations of their corresponding communicative functions.

1071 **Instructions to Annotators:** You are provided with a communicative function label (e.g.,
 1072 “Emphasis”) and a corresponding gesture description (e.g., “Right hand performs rhythmic beat”).
 1073 Please assess whether the described gesture appropriately fulfills or expresses the given function.

- 1075 • Q1: Is this mapping coherent? (Yes / No)
- 1076 • Q2 (Optional): If you selected ”No”, briefly explain why.

1078 **Evaluation Protocol:** We randomly selected 50 samples and recruited 2 expert annotators. Final
 1079 coherence score is computed as the average percentage of “Yes” responses across raters.

1080 **Study 2: Motion Description-Keyframe Fidelity** **Objective:** Determine whether the motion
 1081 description accurately reflects the visible pose and dynamics presented in the keyframes.
 1082

1083 **Instructions to Annotators:** You are shown a short video segment (or sequence of static keyframes)
 1084 and a motion description (e.g., “Left hand slowly rises while the head turns right”). Please judge
 1085 whether the described motion is clearly and accurately visible in the keyframes.

- 1086 • Q1: Does the motion description match the keyframes? (Yes / Partially / No)
 1087 • Q2 (Optional): If “Partially” or “No”, please explain which aspects were inaccurate or
 1088 missing.
 1089

1090 **Evaluation Protocol:** We used the same 50 annotated samples and had each rated by 2 human
 1091 experts. Final scores are reported as the percentage of samples rated “Yes” (fully correct) and
 1092 “Partially”.
 1093

1094 **Study 3: Inferred Intention Plausibility** **Objective:** Assess whether the inferred communicative
 1095 intention is a reasonable high-level summary of the utterance and accompanying gesture behavior.
 1096

1097 **Instructions to Annotators:** You are shown a spoken utterance (text transcript) and a corresponding
 1098 intention inference (e.g., “The speaker is attempting to reassure the listener about a concern”). Please
 1099 judge whether the intention is plausible based on the content and tone of the utterance.

- 1100 • Q1: Is the inferred intention plausible given the utterance? (Yes / Somewhat / No)
 1101 • Q2 (Optional): If “Somewhat” or “No”, please describe why the inference may be
 1102 overstated or misaligned.
 1103

1104 **Evaluation Protocol:** Each of the 50 samples was evaluated by 2 annotators. We report the
 1105 percentage of “Yes” and “Somewhat” responses to quantify plausibility and over-interpretation.
 1106

1107 D IMPLEMENTATION DETAILS

1109 **Hierarchical Audio-Motion Modality Alignment.** We adopt a dual-tower CLIP-based
 1110 contrastive framework inspired by Tango Liu et al. (2024a), trained using a global InfoNCE loss. A
 1111 key design choice for handling audio-motion modality alignment is the separation into low-level
 1112 and high-level encoders.
 1113

1114 For the audio stream, we represent input as raw waveforms and apply a 7-layer CNN (low-level)
 1115 followed by a 3-layer Transformer (high-level), following the design of Wav2Vec2 (Baevski et al.,
 1116 2020). For motion, we use a 15D representation and employ a 3-layer residual CNN (adapted from
 1117 the Momask Motion Tokenizer (Guo et al., 2024)) and a 3-layer Transformer.

1118 We use a projection MLP to process low-level features and another projection MLP with mean
 1119 pooling for high-level features. Both audio and motion streams are temporally downsampled by a
 1120 factor of 4.

1121 **Local and Global Contrastive Loss.** We retain the InfoNCE loss over CLS tokens for global
 1122 alignment, and additionally introduce a frame-level local contrastive loss. We treat frames within a
 1123 temporal window ($i \pm t$) as positives and distant frames ($i - kt, i - t, i + t, i + kt$) as negatives,
 1124 with $t = 4$ and $k = 4$ under a 30 FPS setting. This localized loss encourages robustness to minor
 1125 temporal misalignments common in natural talking scenarios.

1126 **Stop-Gradient on Low-Level Encoders.** To jointly optimize both low- and high-level represen-
 1127 tations, we stop the gradient flow from the global InfoNCE loss to the low-level encoders, as in
 1128 Tango Liu et al. (2024a). This design promotes complementary feature learning across hierarchy
 1129 levels.
 1130

1131 **Intentional Gesture Tokenization.** We design the motion tokenizer using a simplified version of
 1132 the encoder architecture above, followed by a decoder that mirrors its structure. To stabilize training,
 1133 we reduce both to a single Transformer layer but maintain the same residual CNN blocks. The latent
 1134 feature dimension is set to 512.

We apply a self-attention layer to project the 512-dimensional encoding to 32 dimension for quantization. The quantizer comprises 8 codebooks, with a dimension 32 and 8192 codes. For post-quantization, another attention layer maps the 32D features back to 512D for decoding.

Intentional Gesture Generator. The generator operates on token sequences produced by the tokenizer. It uses a Transformer with DiT Peebles & Xie (2023) architecture with 8 layers, a hidden dimension of 256, and a feedforward dimension of 1024, and number of head to be 4. In each layer, there is one self-attention, one cross-attention and followed with the feed-forward layer. For the cross-attention layer, due to two levels of audio conditioning, we design the structure of **Decoupled Cross-Attention**. Rather than forcing a single attention over mixed features, we apply two cross-attention branches separately. Given a shared query Q , we compute:

$$\mathcal{Z}_r = \text{SoftMax} \left(\frac{QK_r^\top}{\sqrt{d}} + \mathbf{P} \right) V_r, \quad \mathcal{Z}_i = \text{SoftMax} \left(\frac{QK_i^\top}{\sqrt{d}} + \mathbf{P} \right) V_i, \quad (4)$$

where (K_r, V_r) and (K_i, V_i) are key-value pairs from rhythmic and intentional features, respectively. The outputs \mathcal{Z}_r and \mathcal{Z}_i are summed to form the final conditioning representation.

This design introduces only a minimal overhead—adding separate key and value projections (only adding 2% parameters) for each cross-attention layer—yet yields consistent improvements of 0.01–0.03 in FGD across validation runs. This demonstrates the benefit of explicitly modeling disentangled prosodic and semantic cues during gesture generation.

Optimizer Settings. All modules are trained using the Adam optimizer Kingma (2014), with a learning rate of 1×10^{-4} , $\beta_1 = 0.5$, and $\beta_2 = 0.999$. We utilize a liner schedule with constant decay for the learning rate for the model learning. The generator is trained on 800 epoches for both single speaker setting and multi-speaker setting.

E ADDITIONAL EXPERIMENTS

Baseline Methods. We compare against a comprehensive set of recent gesture generation approaches Habibie et al. (2021); Liu et al. (2022a;b; 2023); Chen et al. (2024b); Yi et al. (2023); Liu et al. (2024b); Xu et al. (2024); Liu et al. (2025a), all evaluated under the **1-speaker setting** for fair comparison. This setting is used by most prior works and allows precise alignment with publicly reported results on BEAT-2.

Full Generation Results. Table 10 presents the quantitative results on the BEAT-2 benchmark. Our model, **Intentional-Gesture**, achieves state-of-the-art performance across all key metrics. Notably, our method obtains the lowest FGD (**0.379**), indicating the highest overall realism, while maintaining strong beat consistency (0.690) and natural motion diversity (11.00). These results demonstrate the benefit of our intentional alignment and conditioning mechanisms in generating gestures that are both semantically expressive and rhythmically precise.

Results on Audio2PhotoReal. Table 11 presents the quantitative results on the Audio2PhotoReal Ng et al. (2024) benchmark. Our model, **Intentional-Gesture**, achieves state-of-the-art performance across all key metrics. These results demonstrate the benefit of our intentional alignment and conditioning mechanisms in generating gestures can also be generalizable to dyadic conversational speaking and listening settings.

Effect of Speaker Diversity on Retrieval. To examine how speaker diversity influences model generalization, we fix the total number of training

Table 10: The quantitative results on BEAT-2. We bold the best results.

| Methods | FGD (↓) | BC (→) | Diversity (→) |
|----------------------------------|--------------|--------------|---------------|
| Ground-Truth | — | 0.703 | 11.97 |
| HA2G Liu et al. (2022c) | 1.232 | 0.677 | 8.626 |
| DisCo Liu et al. (2022a) | 0.942 | 0.643 | 9.912 |
| CaMN Liu et al. (2022b) | 0.664 | 0.676 | 10.86 |
| DiffSHEG Chen et al. (2024b) | 0.714 | 0.743 | 8.21 |
| TalkShow Yi et al. (2023) | 0.621 | 0.695 | 13.47 |
| ProbTalk Liu et al. (2024b) | 0.504 | 0.771 | 13.27 |
| EMAGE Liu et al. (2023) | 0.551 | 0.772 | 13.06 |
| Audio2PhotoReal Ng et al. (2024) | 1.02 | 0.550 | 12.47 |
| ManbaTalk Xu et al. (2024) | 0.536 | 0.781 | 13.05 |
| SynTalker Chen et al. (2024a) | 0.469 | 0.736 | 12.43 |
| GestureLSM Liu et al. (2025a) | 0.409 | 0.714 | 13.24 |
| Intentional-Gesture | 0.379 | 0.690 | 11.00 |

Table 11: The quantitative results on Audio2PhotoReal. We bold the best results.

| Methods | FGD (↓) | Diversity (→) |
|----------------------------------|-------------|---------------|
| Ground-Truth | — | 2.50 |
| EMAGE Liu et al. (2023) | 4.43 | 2.13 |
| Audio2PhotoReal Ng et al. (2024) | 2.94 | 2.36 |
| GestureLSM Liu et al. (2025a) | 2.64 | 2.34 |
| Intentional-Gesture | 2.21 | 2.43 |

Table 12: **Ablation on Speaker Diversity.** Increasing speaker diversity consistently boosts retrieval for both seen (*Known*) and unseen (*Unknown*) speakers, indicating better generalization.

| Num | Known | | | Unknown | | |
|-----|-------|-------|-------|---------|------|-------|
| | R@1↑ | R@5↑ | R@10↑ | R@1↑ | R@5↑ | R@10↑ |
| 1 | 20.63 | 40.34 | 50.67 | 1.03 | 1.95 | 2.56 |
| 2 | 29.41 | 57.63 | 60.61 | 1.44 | 2.31 | 2.78 |
| 3 | 31.37 | 60.42 | 63.39 | 1.67 | 2.49 | 2.92 |
| 4 | 33.52 | 63.52 | 66.87 | 1.87 | 2.64 | 3.01 |

samples and vary only the number of distinct speakers contributing data. As shown in Tab. 12 (right), increasing the number of training speakers from 1 to 4 significantly improves retrieval performance across both **in-domain** (seen speakers) and **out-of-domain** (unseen speakers) settings.

Notably, for in-domain cases, Recall@1 rises from 20.63% (1 speaker) to 33.52% (4 speakers), while for out-of-domain speakers, Recall@1 improves from 1.03% to 1.87%. These gains indicate that speaker diversity not only enriches the representation space but also enables more robust cross-speaker generalization. We hypothesis that training with a wider range of gestural patterns allows the model to better disentangle speaker-specific motion from shared semantic-rhythmic alignment.

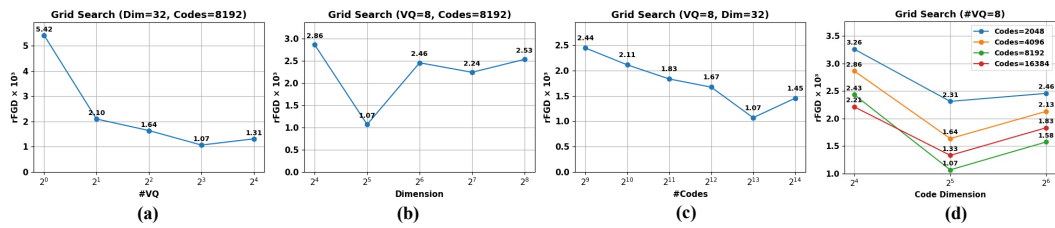


Figure 9: **Tokenizer ablation.** We perform both global and local grid searches to study the effects of codebook design choices on rFGD ($\times 10^3$). (a)–(c): Global sweeps varying one factor at a time; (d): Local grid search over code count and dimension. All results confirm consistent trends: 8 codebooks, a code dimension of 32, and 8192 codes yield optimal or near-optimal performance.

Design Analysis. We ablate design choices of the tokenizer, including the number of codebooks, code dimension, and code size. Fig. 9 shows that (1) 8 codebooks outperform fewer or more, balancing representational capacity and model compactness; (2) a code dimension of 32 achieves the best trade-off between expressiveness and compression; and (3) increasing code size improves rFGD up to 8192 codes, with diminishing returns beyond. These trends are consistent across global and local grid searches. For architecture design, we discover CNN presents better reconstruction quality, but the transformer presents better generation FGD. Our hybrid design takes the advantage of both variants.

Long Sequence Generation Quality. In the main paper, the experiment setting were conducted to generate sequences for the whole testing sequence. Specifically, we follow the existing works Liu et al. (2023; 2025a); Chen et al. (2024b) to utilize a sliding window for long sequence generation (with an average of 65.66 seconds). Each time, we provide the previous 2.13 seconds (a sequence length of 16 for neural representation) generated from the previous generated segment as the condition for the current time segment. Naturally, this setting is easy to encounter the error propagation issue (if the sequence from the previous generation present low quality, this error will be propagated to the current time segment). To understand this effect, we further design the new setting that replicate the inference setting of the same inference audio length as that utilized during training (8.633 seconds). We present the comparison setting between EMAGE, GestureLSM and Intentional-Gesture for single speaker setting in Tab.13. On long sequences, our model achieves the best performance (FGD = 0.379, BC = 0.690, Div. = 11.00). Under short-sequence inference, our FGD further improves by 0.133 (to 0.246), closely matching the improvements of 0.140 and 0.107 seen for EMAGE and GestureLSM, respectively—indicating a consistent FGD gap of 0.12 across models. Note that BC is not reported (–) for 8.633 s segments, due to the tricky implementation to select the precise audio segments from full ground-truth sequences with the generation segments. These results underscore the impact of error accumulation in sliding-window co-speech gesture generation and motivate future work on mitigating segment-wise propagation.

1242 Table 13: Comparison of long-sequence (full test sequences) vs. short-sequence (8.633 s) inference
 1243 on the single-speaker setting.

| | Long-seq Generation | | | Short-seq Generation | | |
|-------------------------------|---------------------|--------------|--------------|----------------------|-------|--------------|
| | FGD↓ | BC→ | Div.→ | FGD↓ | BC→ | Div.→ |
| <i>Single-speaker</i> | | | | | | |
| GT | 0.703 | 11.97 | | 0.703 | 11.97 | |
| EMAGE Liu et al. (2023) | 0.570 | 0.793 | 11.41 | 0.430 | - | 9.57 |
| GestureLSM Liu et al. (2025a) | 0.408 | 0.714 | 13.24 | 0.301 | - | 12.12 |
| Ours | 0.379 | 0.690 | 11.00 | 0.246 | - | 10.21 |

1250 **Quantizer Comparisons Analysis** To isolate the influence of architecture on tokenizer performance,
 1251 we standardized all encoder-decoder backbones to our CNN+Transformer design, which
 1252 we found consistently outperforms alternatives across various quantizers. Specifically:

- 1253 (1) EMAGE Liu et al. (2023) originally uses separate VQ quantizers for upper body, lower body, and
 1254 hands. We replace its CNN encoders with our ResNet-style CNN blocks and normalize codebook
 1255 embeddings rather than using raw outputs. We keep the original codebook size and dimensionality
 1256 to demonstrate how reducing dimension and increasing code count affects performance.
- 1257 (2) For RAG-Gesture Mughal et al. (2025), we re-implement their encoder and decoder based on
 1258 Latent Motion Diffusion from MotionLCM codebase Dai et al. (2024). The comparisons indicates
 1259 for the continuous representation, it is hard to present the motion latent with a compressed latent
 1260 mean prediction from VAE encoder to ensure it is synchronized with the audio for generation.
- 1261 (3) For ProbTalk Liu et al. (2024b), we maintain their design of product quantization while improve
 1262 the encoder and decoder with our design. This comparison indicates the product quantization, while
 1263 present a latent codebook split, unlike our codebook design of separate latent motion representation,
 1264 presents an inferior performance.
- 1265 (4) For GestureLSM Liu et al. (2025a), we maintain the design of 6 layers of codebooks for
 1266 each body region (upper, lower and hands), which leads to 18 codebook in total. While this
 1267 multi-codebook approach achieves competitive reconstruction, its reliance on separate decoders for
 1268 sequential region generation reduces efficiency and harms overall motion quality.

F USER STUDY DETAILS

1273 For user study, we recruited 20 participants with good English proficiency. To conduct the user
 1274 study, we randomly select videos from GestureLSM Liu et al. (2025a), EMAGE Liu et al. (2023),
 1275 CAMN Liu et al. (2022b) and ours. Each user works on 8 videos. The users are not informed of the
 1276 source of the video for fair evaluations. A visualization of the user study is shown in Fig 10.

G METRIC DETAILS

1280 **Fréchet Gesture Distance (FGD).** We adopt Fréchet Gesture Distance Yoon et al. (2020) to
 1281 quantify the distributional similarity between real and generated gestures. Inspired by FID in
 1282 image generation, FGD compares mean and covariance statistics of latent features extracted from a
 1283 pretrained network:

$$FGD = \|\mu_r - \mu_g\|^2 + \text{Tr} \left(\Sigma_r + \Sigma_g - 2(\Sigma_r \Sigma_g)^{1/2} \right), \quad (5)$$

1288 where (μ_r, Σ_r) and (μ_g, Σ_g) are the empirical means and covariances of real and generated gesture
 1289 embeddings, respectively. Lower FGD indicates better realism and distributional alignment.

1290 **L1 Diversity (Div.).** To assess sample-level variation, we compute L1 Diversity Li et al. (2021a),
 1291 defined as the average pairwise L1 distance across N generated sequences:

$$\text{L1 Diversity} = \frac{1}{2N(N-1)} \sum_{t=1}^N \sum_{j=1}^N \left\| p_t^i - \hat{p}_t^j \right\|_1, \quad (6)$$

1296

1297

1298

1299

1300

1301

1302

1303

1304

1305

1306

1307

1308

1309

1310

1311

1312

1313

1314

1315

1316

1317

1318

1319

1320

1321

1322

1323

1324

1325

1326

1327

1328

1329

1330

1331

1332

1333

1334

1335

1336

1337

1338

1339

1340

1341

1342

1343

1344

1345

1346

1347

1348

1349

Subjective Evaluation of Video Generation Quality

Thank you for participating in the evaluation.

Instructions:

Please watch each gesture video and rate the videos based on Three evaluation metrics,

1. Realness: How real the gesture is
2. Synchronization: Whether the gesture is synchronized with the audio
3. Smoothness: Whether the gesture is smooth and natural

Please rate each video on a scale of 1 to 5, where 1 is the lowest and 5 is the highest

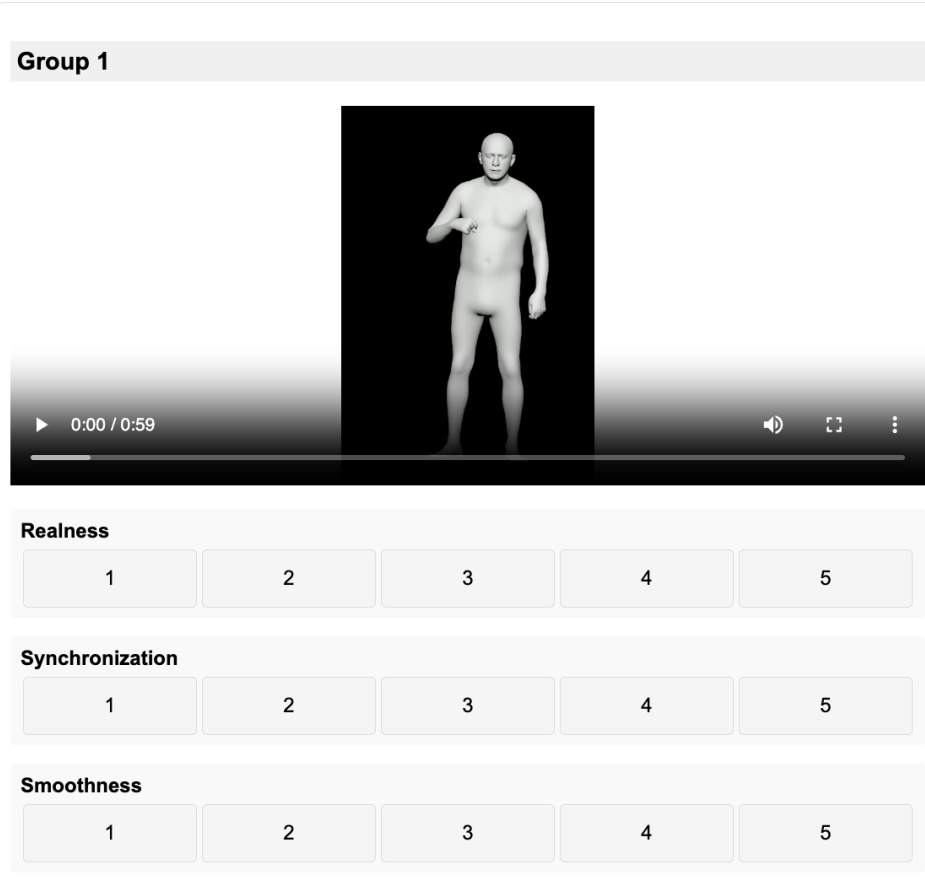


Figure 10: User Study Screenshot

where p_t^i and \hat{p}_t^j denote the joint positions at frame t for the i -th and j -th sequences. To focus on local articulation, global translation is removed before computing distances.

Beat Constancy (BC). Beat Constancy Li et al. (2021b) measures rhythmic alignment between gesture dynamics and speech. Motion beats are detected as local minima in upper body joint velocity, while speech onsets define audio beats. BC is computed as:

$$\text{BC} = \frac{1}{|g|} \sum_{b_g \in g} \exp \left(-\frac{\min_{b_a \in a} \|b_g - b_a\|^2}{2\sigma^2} \right), \quad (7)$$

where g and a are the sets of gesture and audio beats, respectively. BC closer to ground-truth implies stronger gesture-speech synchronization.

1350 **H ETHICAL STATEMENT**

1351

1352 While our work is centered on generating human motion videos, it raises ethical concerns due to
 1353 its potential misuse for photorealistic human motion retargeting. We emphasize the importance
 1354 of responsible use and recommend implementing practices such as watermarking and deepfake
 1355 detection to mitigate the risks involving deepfake videos and animated representations.

1356

1357 **I REPRODUCIBILITY STATEMENT**

1358

1359 We have provided the code of algorithmic annotation for the motion pattern analysis in the
 1360 supplementary material together with the code for the whole system.

1361

1362 **J THE USE OF LARGE LANGUAGE MODELS**

1363

1364 We utilize Large Langauge Models for the dataset annotation and paper polishing.

1365

1366 **K LIMITATIONS**

1367

1369 While our framework demonstrates strong performance across alignment, tokenization, and gesture
 1370 generation, several limitations remain.

1371

1372 First, our method relies on pre-annotated sentence-level intention descriptions to guide semantic
 1373 learning. This setup assumes that such annotations are either available or can be reliably extracted,
 1374 which may not hold in less curated or low-resource scenarios. Future work could explore
 1375 unsupervised or weakly supervised intention discovery to broaden applicability.

1376

1377 Second, while the multi-codebook tokenizer introduces structure into the latent space, it does not
 1378 guarantee complete disentanglement between semantic and rhythmic dimensions. Investigating
 1379 more principled inductive biases or factorized token learning may improve interpretability and
 controllability.

1380 Third, as shown in Sec.E, we discover that existing methods present error propagation issues for
 1381 long-sequence generation settings. We would like to highlight this issue and hope future works can
 1382 propose solutions for this fundamental issue for the co-speech gesture generation domain.

1383 Fourth, in this work, while the motion description annotation, gesture-behavior function mapping
 1384 are intermediate outputs during the annotation procedure, they are not input as variables for the
 1385 motion control but only intention annotations were utilized. We build this simple baseline because
 1386 during inference procedure, we are not able to obtain these motion relatedness analysis. However,
 1387 we argue that the values of these annotations should not be ignore and hope future works can further
 1388 explore the use cases of these annotations as well for motion control and inspire the analysis of the
 1389 relationships between gesture motion patterns and linguistic cues from speech context.

1390 Finally, although our hierarchical alignment improves generalization across speakers, domain
 1391 shifts—such as significant accent variation, disfluency, or cultural gesture norms—remain challeng-
 1392 ing. Incorporating domain adaptation techniques or cross-cultural gesture modeling could enhance
 1393 robustness in real-world deployments.

1394
 1395
 1396
 1397
 1398
 1399
 1400
 1401
 1402
 1403